



Wound healing potential of antibacterial microneedles loaded with green tea extracts



So Young Park ^{a,1}, Hyun Uk Lee ^{a,*,1}, Young-Chul Lee ^{b,1}, Gun Hwa Kim ^c, Edmond Changkyun Park ^c, Seung Hyun Han ^d, Jeong Gyu Lee ^d, Saehae Choi ^e, Nam Su Heo ^f, Dong Lak Kim ^a, Yun Suk Huh ^g, Jouhahn Lee ^{a,**}

^a Division of Materials Science, Korea Basic Science Institute (KBSI), Daejeon 305-333, Republic of Korea

^b Department of BioNano Technology, Gachon University, 1342 Seongnamdaero, Sujeong-gu, Seongnam-si, Gyeonggi-do 461-701, Republic of Korea

^c Division of Life Science, Korea Basic Science Institute (KBSI), Daejeon 305-333, Republic of Korea

^d Small Lab Co., Ltd., Daejeon 305-509, Republic of Korea

^e College of Pharmacy, Chungbuk National University, Cheongju 361-763, Republic of Korea

^f R&D Center, Sugentech, Inc., Daejeon Bioventure Town 461-8, Daejeon 305-811, Republic of Korea

^g Department of Biological Engineering, College of Engineering, Inha University, Incheon 402-751, Republic of Korea

ARTICLE INFO

Article history:

Received 29 March 2014

Received in revised form 13 May 2014

Accepted 16 June 2014

Available online 23 June 2014

Keywords:

Microneedles

Hyaluronic acid

Green tea extract

Transdermal drug delivery

Antibacterial activity

Wound healing

ABSTRACT

This study evaluates the utility of an antibacterial microneedle composed of green tea (GT) extract and hyaluronic acid (HA), for the efficient delivery of GT. These microneedles have the potential to be a patient-friendly method for the conventional sustained release of drugs. In this study, a fabrication method using a mold-based technique to produce GT/HA microneedles with a maximum area of ~50 mm² with antibacterial properties was used to manufacture transdermal drug delivery systems. Fourier transform infrared (FTIR) spectrometry was carried out to observe the potential modifications in the microneedles, when incorporated with GT. The degradation rate of GT in GT/HA microneedles was controlled simply by adjusting the HA composition. The effects of different ratios of GT in the HA microneedles were determined by measuring the release properties. In HA microneedles loaded with 70% GT (GT70), a continuous higher release rate was sustained for 72 h. The in vitro cytotoxicity assays demonstrated that GT/HA microneedles were not generally cytotoxic to Chinese hamster ovary cells (CHO-K1), human embryonic kidney cells (293T), and mouse muscle cells (C2C12), which were treated for 12 and 24 h. Antimicrobial activity of the GT/HA microneedles was demonstrated by ~95% growth reduction of gram negative [*Escherichia coli* (*E. coli*), *Pseudomonas putida* (*P. putida*), and *Salmonella typhimurium* (*S. typhimurium*)] and gram positive bacteria [*Staphylococcus aureus* (*S. aureus*) and *Bacillus subtilis* (*B. subtilis*)], with GT70. Furthermore, GT/HA microneedles reduced bacterial growth of infected wound sites in the skin and improved wound healing process of skin in rat model.

© 2014 Elsevier B.V. All rights reserved.

1. Introduction

Transdermal delivery systems using microneedles with antibacterial properties are used for controlled, consistent, and pain-free administration of therapeutic drugs to a patient's skin for wound healing [1–3]. Microneedle arrays are needle-like structures with diameters in the order of microns, which are used to disrupt the outer layers of the skin to enable (trans)dermal drug delivery [4]. Microneedle arrays have been developed using various materials, including silicon [5], glass [6], metal [7], and polymers [8], and with a variety of shapes and sizes, as needed for different applications. However, silicon, glass and

metal, microneedles can result in sharp bio-hazardous wastes with immunogenic consequences. Among these materials, biodegradable polymer microneedles are also of interest for (trans)dermal drug delivery due to their enhanced biocompatibility and capability to encapsulate the drug within the microneedle matrix [9,10]. Various materials such as sugars [11] and water-soluble polymers [10] have been used to fabricate dissolvable microneedles. In these cases, the microneedles gradually dissolve or degrade in the skin, releasing the loaded drugs, and the dressing materials can be easily removed after the healing process [12,13]. Compared to coated microneedle systems, dissolvable microneedles can incorporate large amounts of drugs and prevent potential immunogenic reactions to the microneedles during drug delivery [14–16].

One of the approaches to treat various types of wound infections is to reduce the bacterial load in the wound [17,18]. An infection can seriously delay wound healing. As an antibacterial agent, green tea (GT)

* Corresponding author. Tel.: +82 42 865 3637; fax: +82 42 865 3610.

** Corresponding author. Tel.: +82 42 865 3613; fax: +82 42 865 3610.

E-mail addresses: leeho@kbsi.re.kr (H.U. Lee), jouhahn@kbsi.re.kr (J. Lee).

¹ These authors contributed equally to this work.

extract has drawn considerable attention owing to its ability to prevent infections. The major compounds present in GT include polyphenols, which are potent antibacterial, anti-carcinogenic, anti-viral, anti-allergic, and anti-inflammatory agents [19,20]. Catechins present in GT have shown inhibitory effects on gram-positive and gram-negative bacteria by disrupting cell membranes and decomposing essential metabolites [19–22].

Here, we report the fabrication of bio-polymer (hyaluronic acid; HA)-based large-area microneedles in different shapes/formats, which facilitate the loading and release of GT for controlled antibacterial molecule delivery. Our dissolvable microneedle arrays are composed of HA as the base material. As HA is a polysaccharide, which is commonly present in most species and localized in multiple sites of the human body, including the skin and soft tissue, it is a safe exogenous material for insertion. In addition, its low cost, biodegradability, and non-polluting nature make it a suitable candidate for wound dressing [23, 24]. These HA microneedles loaded with green tea extract (GT/HA) can be an attractive approach for topical treatment of skin infections by the minimally invasive delivery of antimicrobial molecules. GT has a strong capability to kill bacteria, and its activity persists even when it is incorporated into a polymer matrix. The major functional advantage of GT/HA microneedles is the reduction of bacterial colonization. They provide a safe barrier to protect the wound from further physical damages and any contaminations from exogenous organisms. In addition, the molding processes make it easy to impregnate the various structures of microneedles with antibacterial or therapeutic agents. These systems are superior to conventional microneedle systems with controllable drug delivery and have significant potential for novel clinical applications.

2. Experimental section

2.1. Preparation of GT

Dried GT leaves before chemical treatment were purchased from Boseong Co. Ltd., Korea. The GT leaves were steamed and parched after picking to prevent oxidation of the catechins as the main compound present in the leaf. The dried leaves (100 g) were mixed with distilled water (DI water; 1 L) and heated at 80 °C for 30 min with continuous stirring, followed by the addition of absolute ethanol (300 mL) at room temperature to give 24 h extraction. The decanted

supernatant was filtered twice through Whatman® No. 4 filters. The GT solution was placed in a freezer at $-80\text{ }^{\circ}\text{C}$ for one day and then dried in a freeze dryer ($-42\text{ }^{\circ}\text{C}$, below $133 \times 10^{-3}\text{ mbar}$) for 48 h. After freeze-drying, the samples were pulverized to obtain a powdered form.

2.2. Fabrication of GT/HA microneedles

Fig. 1 illustrates the process employed to fabricate GT/HA microneedles for wound healing. HA and green tea extract (GT) were mixed in DI water for more than 0.5 h at room temperature to obtain mixtures at different ratios of GT [0% (HA), 10% (GT10), 30% (GT30), 50% (GT50) and 70% (GT70)]. The mixed solution was cast on the master at high pressure to remove bubbles. Then, the solution was loaded into the press mold by drop casting. Dissolvable GT/HA mixture microneedles were created via in situ polymerization of liquid monomer within a press mold. The consistent pressing force is 2 kgf/cm² at a temperature of 50 °C for 5 min. During the casting process, the mixture was continuously compressed to minimize void formation. The microneedles were then heated for crosslinking (press) and hardened in a dry oven at 60 °C for 2 h. The cured GT/HA microneedles were subsequently peeled from the master structures. Finally, the GT/HA microneedle array was gently peeled out of the mold.

2.3. Characterization of GT/HA microneedles

Arrays of $50 \times 50\text{ mm}^2$ wedge type microneedles were made with 250 μm radius tips, and 500 μm height (tip-to-tip distance of all samples was 1 mm). The resulting GT/HA microneedles were examined using a scanning electron microscope (SEM, Hitachi S-4000, Tokyo, Japan). Fourier transform infrared (FTIR) spectrometry was carried out to observe the structural interactions of microneedles incorporated with GT. The FTIR spectra of GT/HA microneedle were recorded from 400 to 4000 cm^{-1} at a resolution of 1 cm^{-1} using a Nicolet Magna IR 550 FTIR spectrometer (Nicolet Instrument Corporation, Madison, WI, USA).

2.4. Antibacterial biomolecules release test of GT/HA microneedle into the liquid culture medium

To quantify the release kinetics of GT/HA microneedles [25], samples were prepared by the immersion of microneedles of different GT

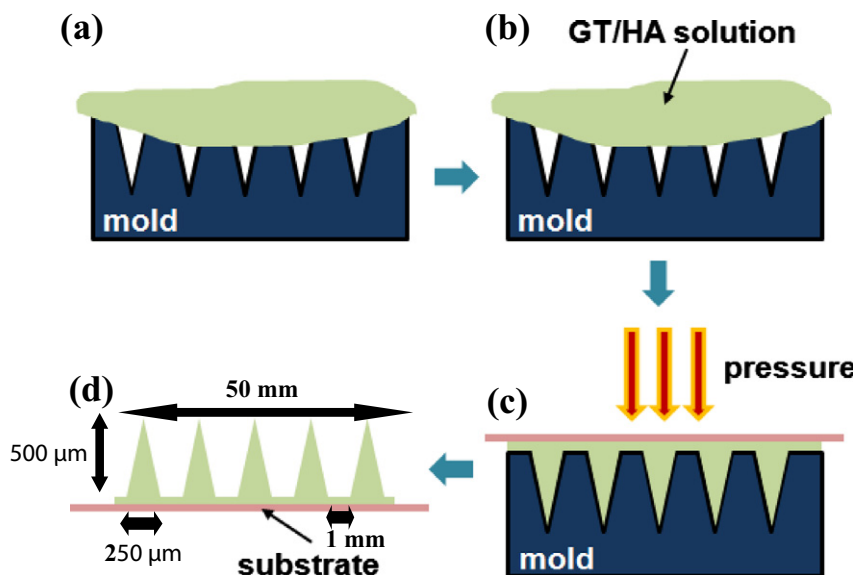


Fig. 1. Illustration of the fabrication process for biodegradable microneedles. (a) preparation of press mold, (b) cover of green tea extract and hyaluronic acid (GT/HA) solution, (c) filling of GT/HA solution in the cavities of press mold using master structure, and (d) GT/HA microneedles peeled from the master structures.

concentrations (0%, 10%, 30%, 50% and 70%) in 100 mL phosphate buffer solution (PBS) for a period of time. The vials were magnetically stirred at 500 rpm and incubated in a water bath at 37 °C. The GT/HA microneedles were cut into 25 × 25 mm sections. Once each time point was reached, the microneedles were removed from the PBS to stop further release of GT. Samples were incubated at 37 °C. The GT released into the solution was determined by monitoring the absorbance at 277 nm using a UV–Visible spectrophotometer (Cary 50, Varian Inc., USA) at selected time intervals.

2.5. Cytotoxicity analysis of GT/HA microneedle

According to the literature [25], the Chinese hamster ovary cells (CHO-K1), human embryonic kidney cells (293T), and mouse muscle cells (C2C12) were grown in Dulbecco's Modified Eagle Medium (DMEM) or Roswell Park Memorial Institute (RPMI) supplemented with 10% fetal bovine serum (FBS), 5% penicillin and maintained in a humidified atmosphere of 5% CO₂ at 37 °C. The cells were seeded in a 6 well tissue-culture plates, at a concentration of 1×10^5 cells/mL in complete DMEM or RPMI, and incubated for 24 h for cell stabilization. Media of cells were treated with GT/HA microneedles (radius ~35 mm), and incubated for 24 h in a humidified atmosphere of 5% CO₂ at 37 °C. For cytotoxicity test, the neutral red uptake assay method was employed. The cells were washed with 2 mL PBS buffer per well, and 2 mL neutral red (3-amino-7-dimethylamino-2-methyl-phenazine hydrochloride, Sigma, cat. no. N4638) medium was added to each well of the plate and incubated on a shaker for 1 h at 37 °C. The cells were washed with 2 mL PBS buffer per well and 1 mL destain solution was added in each well. The plates were shaken on a microtiter plate shaker for 10 min, to facilitate the extraction of neutral red from the cells. The density of neutral red extract was measured using the optical density (OD) at 540 nm in a microtiter plate-reader spectrophotometer.

2.6. Bacterial culture for antimicrobial tests of GT/HA microneedle

According to the literature [26], bacterial strains, which include 3 gram-negative strains, *Escherichia coli* (*E. coli*; KCTC1041), *Salmonella typhimurium* (*S. typhimurium*; KCTC2054), and *Pseudomonas putida* (*P. putida*; KCTC1134) and 2 gram-positive strains, *Bacillus subtilis* (*B. subtilis*; KCTC2217) and *Staphylococcus aureus* (*S. aureus*; KCTC1916), were used to test the microbial inactivation. All strains were cultivated in test tubes containing 10 mL Luria-Bertani (LB) medium supplemented with 2% (w/v) glucose at 37 °C in a rotary shaking incubator. Then, the bacterial cells in the culture were mixed with GT/HA microneedles (radius ~35 mm). The test tube was incubated at 37 °C for 24 h. The cells were diluted to 1×10^5 using a serial dilution method. The prepared 500 µL suspension of 4 microorganisms (*E. coli*, *S. typhimurium*, *B. subtilis*, *S. aureus*, and *P. putida*) was spread onto the LB agar plate, dried in the clean bench, and incubated at 37 °C for 16 h. The number of live microorganisms was monitored.

2.7. In vivo infection and wound healing assay

Animal infection and wound healing experiments were performed with minor modification [27,28]. 8 week-old male Sprague–Dawley rats were anesthetized by intraperitoneal injection of 300 mg/kg of Tribromoethanol (Avertin). The fur was stripped from the rat with hair clippers and Veet® hair removal cream (Reckitt Benckiser, Berkshire, UK). For skin wounding, six round, 4 mm in diameter, full thickness excisions were made on the back of each rat using disposable biopsy punches (Kai Medical, Japan). Bacterial infection was initiated by placing on the skin wounds a 10 µL droplet containing 1×10^7 *P. putida* bacteria concentrated from an overnight bacterial culture in stationary phase. Then, the GT/HA microneedles were placed on the infected skin wounds. For the negative control, sterilized gauze was

put on either the infected or non-infected skin wounds. Three days after wounding and infection, the rats were killed and the areas of skin wounds were measured. Immediately after the rats were killed, the skin wounds, approximately 1 cm², were excised and homogenized in 1 mL of PBS buffer. Suitable dilutions of the homogenates were plated on LB agar plates to determine the number of living bacteria (CFU).

3. Results and discussion

3.1. Characterization of GT/HA microneedles

The SEM results indicated that the GT/HA microneedles have 250 µm radius tips, were 500 µm in height, and the center-to-center spacing was 500 µm (Fig. 2). These microneedles were created by molding and replicating master structures. In this study, GT/HA microneedles with a trigonal pyramid-shape were chosen because of their superior mechanical strength as compared to conical microneedles [29]. GT aggregation was not observed on the GT/HA microneedles array because the extracted GT is mainly consisted of water-soluble materials such as catechin which can be completely dissolved in aqueous solution without its aggregation. The GT/HA microneedles were of consistent rough-shape and spacing, regardless of the GT constituent, and reflected the dimensions of the mold. The entire array of 120 × 120 microneedles occupies a maximum area of ~50 mm² (Fig. 2d). Both the backing substrate and GT/HA microneedles were designed to be flexible for their use as antibacterial tools in an adhesive patch form.

FTIR spectroscopy was used as a tool to analyze the GT incorporation in HA by measuring the absorbance of wave number range from 400 to 4000 cm⁻¹ at a resolution of 1 cm⁻¹. The FTIR spectra of control and those incorporated with 0%, 10%, 30%, 50%, or 70% of GT are shown in Fig. 3. FTIR spectra revealed that the N–H peak between 3000 and 3500 cm⁻¹ [30], corresponding to stretching vibrations of free hydroxyl and to asymmetric and symmetric stretching of the N–H bonds in amino groups, respectively, was stronger in 0% GT (100% HA) microneedles than in those incorporated with GT. In addition, 2 visible water bands at 1400 cm⁻¹ in 0% GT microneedles, associated with OH in-plane bending, were less discernible in GT-incorporated microneedles. Moreover, there was an obvious broadening of the peak at 1660–1700 cm⁻¹, which could possibly indicate the amide C=O stretch [30]. These peaks became smaller with increasing GT concentrations, indicating that the amine functional groups of HA decreased when incorporated with GT.

In order to evaluate the feasibility of HA as a carrier of GT, microneedles with GT were pre-incubated in PBS. Fig. 4 shows the in vitro GT release profiles of the microneedles that contain different concentrations of GT in HA microneedles, in PBS buffer. The release rate of GT was relatively high in the first few hours, decreased over time, and saturated the releasing percent over approximately 60 h in general. When microneedles were inserted into PBS buffer, the exposed microneedle surface probably dissolved rapidly, leading to an initial fast release. At GT70, a continuously higher release rate was sustained until 72 h. At the highest loading of GT, early fast release behavior was observed due to the rapid dissolution of the microneedles, providing limited control [31,32]. Once the drug-loaded microneedles were immersed in an aqueous solution, diffusion of the “trapped” drug out of surface of microneedles was limited by the drug's solubility capacity in the limited volume of an aqueous solution. As a result, sustained and constant release was achieved beyond 30% of GT loading at an initial time. Low cumulative release was observed with 10% GT loading. The percentage of GT released was largely dependent on the amount of HA incorporated in the microneedles. Longer release durations from microneedles can be achieved by controlling the composition of HA. The release of GT from the microneedles was sustained for at least 72 h. The 70% GT loaded microneedles, which had a higher release rate and longest release period,

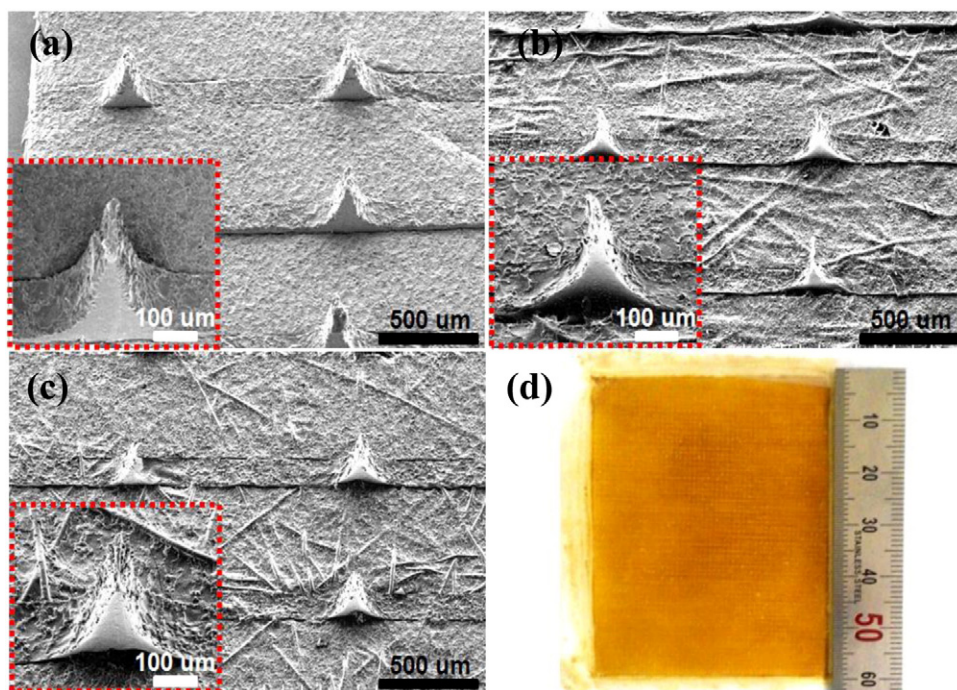


Fig. 2. SEM of (a) HA (GT 0%/HA 100%), (b) GT30 (GT 30%/HA 70%), (c) GT70 (GT 70%/HA 30%), and (d) optical image of GT70 microneedles.

are suitable for long-term wound healing applications. For the effects of shapes and materials of microneedles in release profile [33], sharp microneedles easily penetrate into the skin in order to transport drugs. Thus, wedge types of microneedles had been designed intensively. Dissolving microneedles in this study, which are composed of biocompatible components, is proved to be suitable for wound healing applications.

3.2. Cytotoxicity and antibacterial activities of GT/HA microneedles

GT is widely used as a beverage and its role in traditional medicine has been well documented; it is likely to have minimal toxicity. In order to assess the toxic effects of the manufactured GT/HA microneedles on cells, normal cells (CHO-K1, 293T, and C2C12) were treated with different concentrations of GT. As shown in Fig. 5, the *in vitro* cytotoxicity assays demonstrated that the GT/HA microneedles are not generally toxic to normal cells cultured for 12 h and 24 h. There is no significant difference in cytotoxicity in any of the different concentrations of GT used in this study (Fig. 5). These results indicated that all the prepared GT/HA microneedles are less toxic to normal cells.

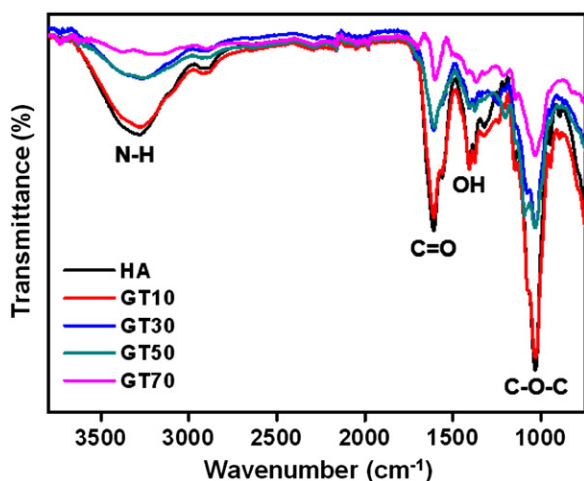


Fig. 3. FTIR spectra of GT/HA microneedles incorporated with GT.

To determine the antibacterial activities of GT/HA microneedles on 5 bacterial strains [3 gram-negative strains (*E. coli*, *S. typhimurium*, and *P. putida*; KCTC1134) and 2 gram-positive strains (*B. subtilis* and *S. aureus*)], GT/HA microneedles with different amounts of GT were prepared and exposed to a bacterial suspension for 24 h at 37 °C (Fig. 6). Surviving cells were harvested from the surface and grown on agar plates for the assessment of colony forming units (CFUs). All bacteria grew very well under control conditions and when exposed to HA microneedles, as observed on the agar plates (inset of Fig. 6). In point of visual approach, as increase in GT content, the clear zone of GT30 and GT70 was compared against *E. coli*. For all tested bacteria, a growth reduction was observed with increasing microneedle GT content. Most significantly, the growth of pathogenic bacteria (*E. coli*, *B. subtilis*, *P. putida*, *S. Aureus*, and *S. typhimurium*) was inhibited even at lower GT content; the bacteria were killed in the presence of GT10 microneedles. Fig. 6 indicates that up to 95% reduction in CFU of pathogenic bacterium type occurred, starting from 70% of GT concentration. The reason for this bactericidal activity is probably due to the catechins

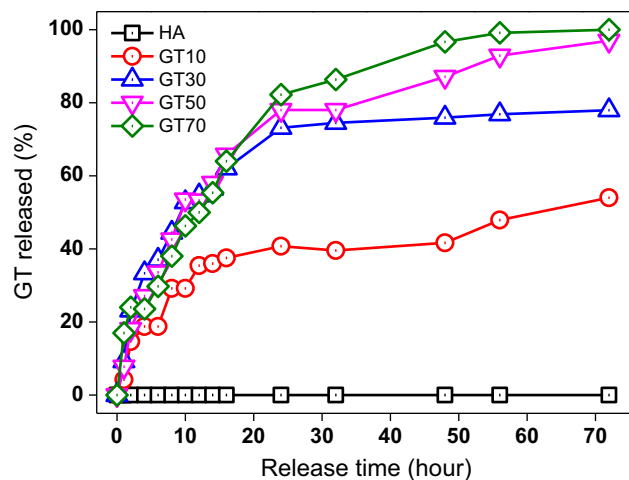


Fig. 4. In vitro drug release profiles for 72 h after loading HA microneedles with different concentrations of GT.

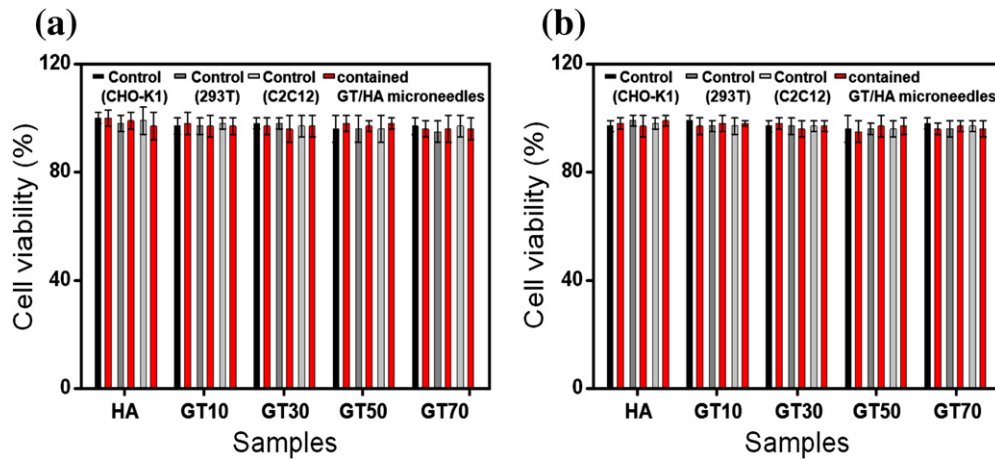


Fig. 5. In vitro cytotoxicity results of GT/HA microneedles for (a) 12 and (b) 24 h. Values in bar graphs are mean \pm s.d. of three independent experiments. The data were averaged and expressed as mean \pm standard deviation. Each test was replicated three times. Statistical analysis was performed using analysis of variance (ANOVA) in which $p < 0.05$ was considered as significant.

of GT in microneedles, which are a group of flavonoids that appear to have greater activity against all bacteria (gram-positive than gram-negative bacteria), and primarily act on and damage the bacterial cell wall and membranes by perturbing the lipid bilayers, possibly by directly penetrating them and disrupting the barrier function.

3.3. Effect of GT/HA microneedles on animal infection model

Finally, to investigate the effect and potential use of GT/HA microneedles in vivo, wound skin and infection assays were performed using rat animal model as shown in Figs. 7, S1 and S2. Skin wounds were made on the back side of rats and bacterial infection was initiated by dropping 1×10^7 CFU of *P. putida*. Then the infected wound skin sites were covered with either GT/HA microneedles or sterilized gauze. Three days after wounding and bacterial infection, the area of wound sites and number of bacteria recoverable from the wounds were determined.

The number of CFU recoverable from the wounds after infection of *P. putida* was $6.18 \pm 0.54 \log_{10}$ (Figs. S1 and S2). When the GT/HA microneedles were placed on the infected wound skin sites, bacterial infection was significantly suppressed. The number of CFU recoverable from the infected skin wounds was $4.24 \pm 0.23 \log_{10}$ from that of treated with GT30 microneedle and $2.03 \pm 0.10 \log_{10}$ from that of treated with GT50 microneedle (Figs. S1 and S2). In the process of wound healing, bacterial infection to skin wounds led to a significant delay in the closure of excisional wound sites compared with non-infected wound sites. When GT/HA microneedles were used to treat the infected wound skin sites, however, wound healing process was dramatically accelerated. The wound area treated with GT30 microneedle was comparable with that of non-infected wound. Moreover, treatment of GT50 showed much greater healing effect. These results indicate that GT/HA microneedle successfully suppresses bacterial growth in the wound skin sites and improves wound healing process. However, GT70 had higher GT concentration than GT50, it exhibited lower wound healing properties than that of GT50; this was attributed to the decrease in the attachment interaction between skin and microneedle by increase of GT concentration due to the increase in stiffness of the microneedle. Therefore, it is suggested that GT50 microneedle has a great potential to be used for clinical treatment of wound skin healing.

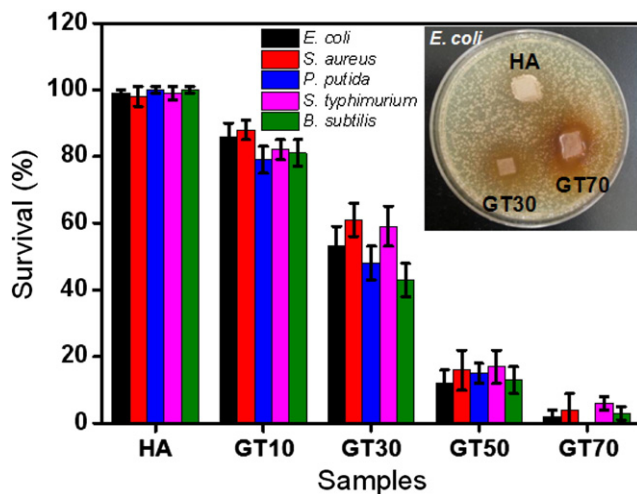


Fig. 6. Antibacterial activity of GT/HA microneedles on 5 bacterial strains [3 gram-negative strains (*Escherichia coli*, *Salmonella typhimurium*, and *Pseudomonas putida*) and 2 gram-positive strains (*B. subtilis* and *S. aureus*)]. Inset shows clear zones for the treatment of GT30, GT70, and HA against *E. coli*. Values in bar graphs are mean \pm s.d. of three independent experiments. The data were averaged and expressed as mean \pm standard deviation. Each test was replicated three times. Statistical analysis was performed using analysis of variance (ANOVA) in which $p < 0.05$ was considered as significant.

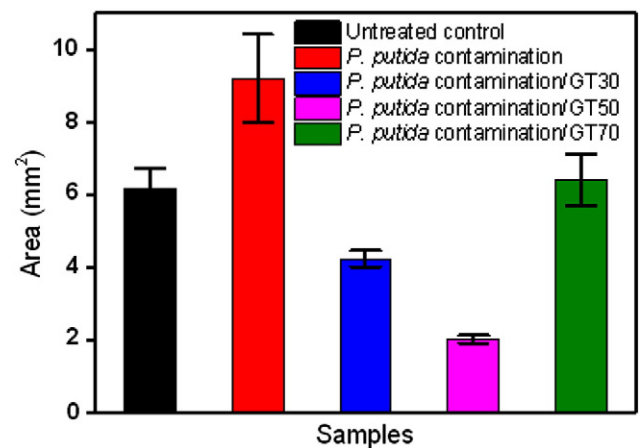


Fig. 7. Wound skin and infection assays of GT/HA microneedles on infection rat's model. Values in bar graphs are mean \pm s.d. of three independent experiments.

4. Conclusion

The antibacterial microneedle-integrated transdermal patch is a reliable approach to improve drug delivery across the skin and prevent infections. The fabrication of antibacterial microneedles was performed using a molding method. In addition, our study indicated that green tea (GT) can be encapsulated within the HA matrix of dissolving microneedles, which has a higher loading capacity. FTIR analysis demonstrated the interactions between functional groups of GT and HA compounds. Our in vitro release study indicated a sustained release of GT from microneedles, with approximately 95% cumulative release observed in 72 h. The microneedles loaded with GT inhibited the growth of bacterial strains and had a potential to prevent local infection of wound skin sites. Moreover, treatment of GT/HA microneedles improves wound skin healing process. The findings of this study suggest that GT/HA microneedles are promising antibacterial tools and may provide a convenient self-administration option for the transdermal delivery of diverse biomolecules.

Acknowledgments

This work (Grant No. PCC238) was supported by the Business for Co-operative R&D between Industry, and Research Institute funded Korea Small and Medium Business Administration in 2012–2014.

Appendix A. Supplementary data

Supplementary data to this article can be found online at <http://dx.doi.org/10.1016/j.msec.2014.06.021>.

References

- [1] K.R. Kam, T.A. Desai, J. Mater. Chem. B 1 (2013) 1878–1884.
- [2] M.R. Prausnitz, R. Langer, Nat. Biotechnol. 26 (2008) 1261–1268.
- [3] K. Maaden, H. Yu, K. Slidregt, R. Zwier, R. Lebourg, M. Oguri, A. Kros, W. Jiskoot, J.A. Bouwstra, J. Mater. Chem. B 1 (2013) 4466–4477.
- [4] Z. Ding, F.J. Verbaan, M. Bivas-Benita, L. Bungener, A. Huckriede, D.J. van den Berg, G. Kersten, J.A. Bouwstra, J. Control. Release 136 (2009) 71–78.
- [5] A. Rodriguez, D. Molinero, E. Valera, T. Trifonov, L.F. Marsal, J. Pallarès, R. Alcubilla, Sensors Actuators B Chem. 109 (2005) 135–140.
- [6] S. Lee, W. Jeong, D.J. Beebe, Lab Chip 3 (2003) 164–167.
- [7] D.G. Koutsouanos, E.V. Vassilieva, A. Stavropoulou, V.G. Zarnitsyn, E.S. Esser, M.T. Taheribhai, M.R. Prausnitz, R.W. Compans, I. Skountzou, Sci. Rep. 2 (2012) 357 (1–10).
- [8] S.P. Sullivan, N. Murthy, M.R. Prausnitz, Adv. Mater. 20 (2008) 933–938.
- [9] S.P. Sullivan, D.G. Koutsouanos, M.D.P. Martin, J.W. Lee, V. Zarnitsyn, S.O. Choi, N. Murthy, R.W. Compans, I. Skountzou, M.R. Prausnitz, Nat. Med. 16 (2010) 915–921.
- [10] J.H. Park, M.G. Allen, M.R. Prausnitz, J. Control. Release 104 (2005) 51–66.
- [11] C.J. Martin, C.J. Allender, K.R. Brain, A. Morrissey, J.C. Birchall, J. Control. Release 158 (2012) 93–101.
- [12] M.Y. Kim, B. Jung, J.H. Park, Biomaterials 33 (2012) 668–678.
- [13] J.W. Lee, J.H. Park, M.R. Prausnitz, Biomaterials 29 (2008) 2113–2124.
- [14] L.Y. Chu, S.O. Choi, M.R. Prausnitz, J. Pharm. Sci. 99 (2010) 4228–4238.
- [15] P.C. DeMuth, Y. Min, B. Huang, J.A. Kramer, A.D. Miller, D.H. Barouch, P.T. Hammond, D.J. Irvine, Nat. Mater. 12 (2013) 367–376.
- [16] P.C. DeMuth, X. Su, R.E. Samuel, P.T. Hammond, D.J. Irvine, Adv. Mater. 22 (2010) 4851–4856.
- [17] E.Y. Teo, S.Y. Ong, M.S.K. Chong, Z. Zhang, J. Lu, S. Mochhala, B. Ho, S.H. Teoh, Biomaterials 32 (2011) 279–287.
- [18] A. Salomé Veiga, C. Sinthuvanich, D. Gaspar, H.G. Franquelim, M.A.R.B. Castanho, J.P. Schneider, Biomaterials 33 (2012) 8907–8916.
- [19] A. Sharma, S. Gupta, I.P. Sarethy, S. Dang, R. Gabrani, Food Chem. 135 (2012) 672–675.
- [20] H.P. Bais, R. Vepachedu, S. Gilroy, R.M. Callaway, J.M. Vivanco, Science 31 (2003) 1377–1380.
- [21] M.P. Almajano, R. Carbo, J.A.L. Jimenez, M.H. Gordon, Food Chem. 108 (2008) 55–63.
- [22] M.V. Staszewski, A.M.R. Pilosof, R.J. Jagus, Food Chem. 125 (2011) 186–192.
- [23] S. Sahoo, C. Chung, S. Khetan, J.A. Burdick, Biomacromolecules 9 (2008) 1088–1092.
- [24] S. Yamane, N. Iwasaki, T. Majima, T. Funakoshi, T. Masuko, K. Harada, A. Minami, K. Monde, S.I. Nishimura, Biomaterials 26 (2005) 611–619.
- [25] C.-J. Ke, Y.-J. Lin, Y.-C. Hu, W.-L. Chiang, K.-J. Chen, W.-C. Yang, H.-L. Liu, C.-C. Fu, H.-W. Sung, Biomaterials 33 (2012) 5156–5165.
- [26] R. Jalal, E.K. Goharshadia, M. Abareschi, M. Moosavi, A. Yousefi, P. Nancarrow, Mater. Chem. Phys. 121 (2010) 198–201.
- [27] P. Gal, R. Kilik, M. Mokry, B. Vidinsky, T. Vasilenko, S. Mozes, N. Bobrov, Z. Tomori, J. Bober, L. Lenhardt, Vet. Med. 53 (2008) 652–659.
- [28] E. Kugelberg, T. Norstrom, T.K. Petersen, T. Duvold, D.I. Andersson, D. Hughes, Antimicrob. Agents Chemother. 49 (2005) 3435–3441.
- [29] M.C. Chen, M.H. Ling, K.Y. Lai, E. Pramudityo, Biomacromolecules 13 (2012) 4022–4031.
- [30] D. Lin, B. Pan, L. Zhu, B. Xing, J. Agric. Food Chem. 55 (2007) 5718–5724.
- [31] K. Tsioris, W.K. Raja, E.M. Pritchard, B. Panilaitis, D.L. Kaplan, F.G. Omenetto, Adv. Funct. Mater. 22 (2012) 330–335.
- [32] M.C. Chen, S.F. Huang, K.Y. Lai, M.H. Ling, Biomaterials 34 (2013) 3077–3085.
- [33] Y.-C. Kim, J.-H. Park, M.R. Prausnitz, Adv. Drug Deliv. Rev. 64 (2012) 1547–1568.